Colloid Polym Sci 273:219–226 (1995)

ORIGINAL CONTRIBUTION

S. Hellinckx
J.-C. Bauwens

The yield behavior of PVDF and the deformation process at high temperature

Received: 22 November 1993
Accepted: 26 April 1994

Prof. Dr. J.-C. Bauwens (✉) · S. Hellinckx
Physique des Matériaux de Synthèse, 194/8
Université Libre de Bruxelles
50 avenue F. Roosevelt
1050 Bruxelles, Belgium

Abstract Tensile yield stress measurement on polyvinylidene fluoride are presented covering as many as seven decades of strain-rates at temperatures from − 50° to 150 °C.

The data have been analyzed on the basis of four Ree–Eyring processes acting in parallel, three of which have been identified.

At high temperatures and low strain-rates, a threshold yield stress is observed. A model is proposed, allowing to describe the yield behavior both at the threshold and in its adjacent strain-rate dependent range. It consists in a modification of the Ree–Eyring theory using an unsymmetrical free energy barrier for the rate process.

The data are fully consistent with the above model which implies that yielding occurs only when the stress is higher than a threshold. In this case, a rejuvenation (or de-aging) effect must be assumed in the deformation process which could consist in a melting of a chain segment located between two folds.

Key words PVDF – yielding – rate process – threshold stress – deformation mechanism – rejuvenation

Introduction

Many workers have used the Ree–Eyring formalism of non-Newtonian viscosity [1] to describe the yield behavior of amorphous [2–5] and some semicrystalline polymers [6, 7] as a function of strain-rate and test temperature. It is proposed that several rate processes, acting in parallel, must be activated at yield so that the yield stress is the sum of the stresses associated with each process. Such processes are related to the different degrees of freedom of a chain segment. They have been associated with damping peaks appearing in the loss curve in the same temperature range and characterized by the same activation energy.

For amorphous polymers, two rate processes are generally involved; the process which is the most important at low temperatures is in fairly good agreement with the β damping peak [8, 9].

Polyvinylidene fluoride (PVDF), a semi-crystalline polymer, is known to exhibit a double glass transition [10]. Two peaks, respectively related to the lower and the upper glass transitions, may be distinguished on the loss curve, as well as other peaks corresponding to molecular motions in both the amorphous and crystalline phases [11–13]. The yield behavior of PVDF has already been investigated in this laboratory [12] over an extensive range of test conditions. The data can be fitted using the Ree–Eyring model and the assumption that three different rate processes are involved. Two rate processes were iden-

tified and associated to the lower and upper glass transitions respectively, but the nature of the third process remained obscure.

The purpose of this paper is to investigate the yield stress at lower strain-rates and higher temperatures, both in tensile and creep tests, in order to throw light upon the long term behavior of PVDF. In such a test condition range, the data reveal the existence of a threshold stress, not implied at all by the Ree–Eyring approach, at which the yield behavior becomes strain-rate independent. Therefore, a modified Ree–Eyring model accounting for a threshold stress is proposed here. The fit to the data, over the whole range explored, is promising, provided one realizes that at least four different rate processes may be involved at yield. Moreover, the higher temperature deformation process is identified.

Previous investigation

Assuming that N processes are involved in the viscous flow occurring at the yield point and that each process i is associated with a single relaxation time, the Ree–Eyring viscosity model [1] leads to the following relation.

$$\frac{\sigma}{T} = \sum_{i=1}^{N} A_i \operatorname{asinh}\left(C_i \dot{\varepsilon} \exp\left(\frac{Q_i}{RT}\right)\right), \tag{1}$$

where $\dot{\varepsilon}$, σ, and T denote the strain-rate, the tensile yield stress and the absolute temperature, respectively, and where A_i, C_i, and Q_i are constant parameters related to process i. When $\sigma \gg A_i T$, the approximation $\sinh(x) \simeq \exp(x)/2$ can be used and Eq. (1) can be rewritten as

$$\frac{\sigma}{T} = \sum_{i=1}^{N} A_i \left(\ln(2C_i\dot{\varepsilon}) + \frac{Q_i}{RT}\right). \tag{2}$$

The tensile yield behavior of PVDF has been investigated previously in this laboratory [12] between $-50°$ and 100 °C over four decades of strain-rates. The data are shown in Fig. 1 where the ratio of yield stress to absolute temperature is plotted against the logarithm of strain-rate. The lines drawn through the data represent the best fit of Eq. (2). The existence of three different processes had to be assumed. The best-fit parameters are given in Table 1.

Figure 2 shows the variation of the yield stress with temperature at constant strain-rate. Two changes in slope may be clearly distinguished respectively related to the onset of process 2 at 50 °C and process 3 at -30 °C; above 50 °C, only process 1 is effective. It must be pointed out that the activation energies related to processes 2 and 3 were found to be equal.

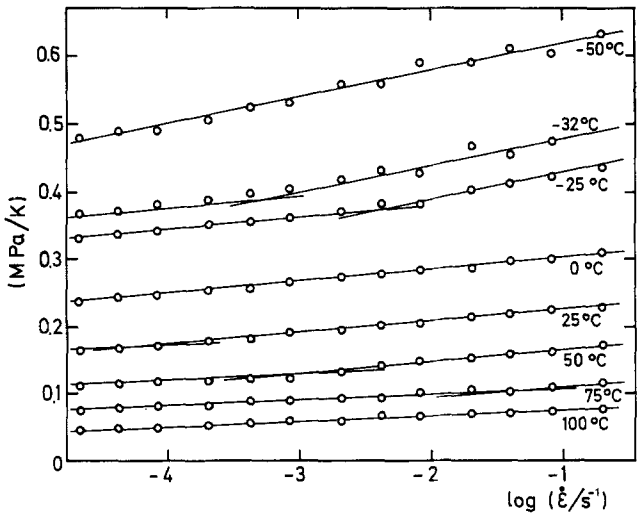

Fig. 1 Ratio of yield stress to absolute temperature versus the logarithm of strain-rate (tensile tests). The curves are calculated from Eq. (2) using the constants given in Table 1

Table 1 Constant parameters related to processes 1, 2 and 3 in PVDF

Process i	A_i(MPa/K)	C_i(s)	Q_i(kJ/mole)
1	$3{,}26.10^{-3}$	4.10^{-51}	435 (apparent)-268 (true)
2	$4{,}2.10^{-3}$	$3{,}3.10^{-22}$	150
3	$9{,}6.10^{-3}$	$2{,}8.10^{-30}$	150

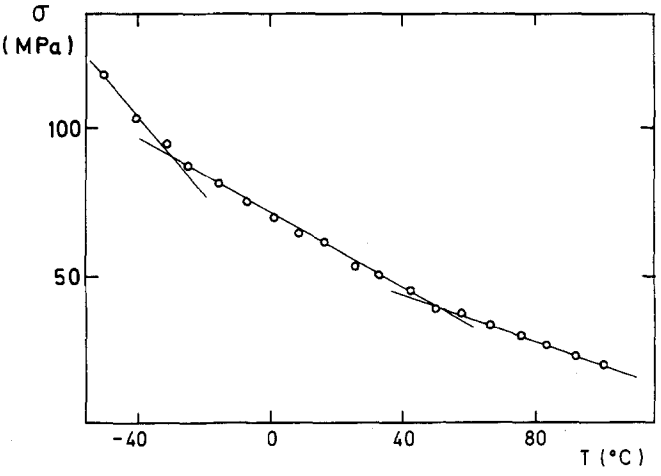

Fig. 2 Yield stress versus temperature at a constant strian-rate of $4{,}17.10^{-4}\,s^{-1}$ (tensile tests). The curves are calculated from Eq. (2) using the constants given in Table 1

Both the position of the yield transition in temperature and the magnitude of the activation energy were in good agreement with mechanical relaxations related to the double glass transition, and therefore, processes 2 and

3 could be associated with the upper and lower glass transitions, respectively.

It was not possible to ascribe any molecular mechanism to process 1, characterized by a high value of the activation energy Q_1.

We intend here to enlarge the investigation above 100 °C over an extended range of strain-rates covering seven decades. The obtained data led us to reanalyze the Q_1 value. It will be shown that Q_1 is an apparent activation energy calculated by assuming that process 1 is a single process while, in fact, it results from two processes only discernible above 100 °C.

Experimental

Samples

Commercially-available PVDF form α(Solex 1010 from Solvay) supplied as extruded sheets was used throughout. The crystallinity χ and the density ρ of the material are listed in Table 2 together with the specific melting enthalpy h of the crystalline phase.

We have checked that the crystallinity remains unchanged over the whole investigated temperature range. No change can be detected even after annealing for 10 h at 150 °C.

The tensile specimens were dumb-bell shaped with a gauge length of 40 mm and 8 × 2 mm cross-section.

Tensile tests

Tensile tests have been performed between 100° and 150 °C on an Instron tensile machine [14] and on a high speed testing machine built in this laboratory. Over the whole range investigated, load-extension curves exhibit a maximum which was taken as the yield point. Engineering stresses were considered throughout. Tensile tests were performed in the Solvay laboratories on samples aged before testing at 165 °C for times varying from 2 to 2000 h. No significant difference was found in the measurements of the yield stress, denoting that no thermal degradation occurs.

Creep tests

In order to investigate the long term behavior, tensile creep tests were performed at 100 °C. Dead weight loading was used inside an environmental chamber. Strain was measured with a dial gauge.

Table 2 Characteristics of PVDF

Characteristic	Unities	Value
χ		0,56
ρ	kg/m^3	1780
h	kJ/kg	109

Results

The results of the tensile yield stress measurements are shown in Fig. 3 where the ratio of yield stress to absolute

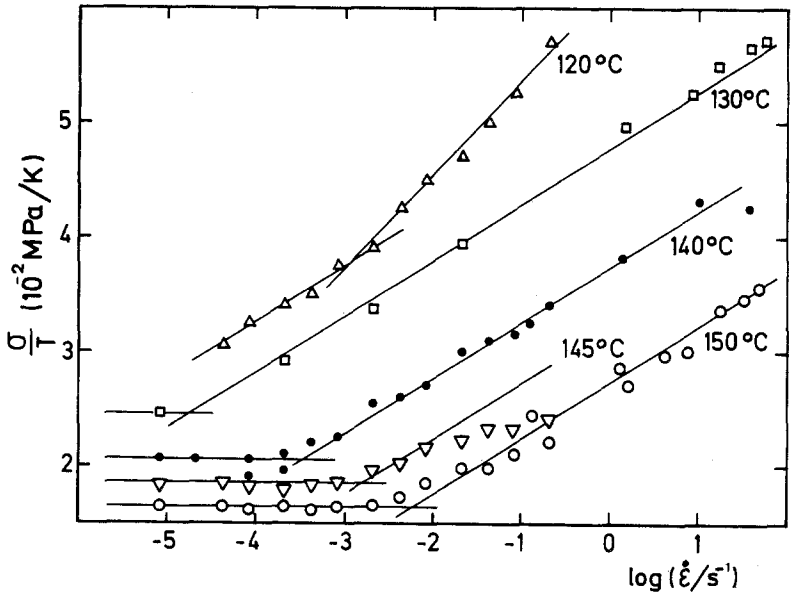

Fig. 3 Ratio of yield stress to absolute temperature versus the logarithm of strain-rate (tensile tests). The threshold curves are calculated from Eq. (11) using the constants given in Table 3 and the curves related to its adjacent strain-rate dependent process are calculated from Eq. (10) using the constants given in Table 3

Colloid & Polymer Science, Vol. 273, No. 3 (1995)

temperature is plotted versus the logarithm of strain-rate at several constant temperatures higher than 100 °C. The lines drawn through the data are theoretical.

At 120 °C and higher strain-rates, the yield behavior may still be related to process 1, already considered previously (see Figs. 1 and 2); but at lower strain-rates, one additional process ought to be assumed. Let us denote it process 0, which governs the high strain-rate yield behavior at temperature up to 150 °C. In Fig. 3, it can be seen that at low strain-rates the yield stress keeps a constant value. It will be shown that this threshold stress may also be related to process 0.

Model

Yield stress data beyond 100 °C reveal the existence of a threshold depending on test temperature, but not on strain-rate (Fig. 3). Now the Ree–Eyring approach, which implies a temperature and strain-rate dependence of yield stress, assumes a symmetrical potential barrier [1] for the deformation process.

To take into account a threshold yield behavior, let us then consider an unsymmetrical barrier, a concept already used in particular by Matz et al. [15]. The free energy curve of a chain segment is represented by Fig. 4 where A and B indicate two neighboring equilibrium positions corresponding to the initial structure and to the structure at the yield point, respectively.

In the absence of an external stress, the probability that yielding occurs is determined by the Maxwell–Boltzmann relationship

$$P_{A\to B} = \exp\left(-\frac{F_{AB}}{RT}\right), \tag{3}$$

where F_{AB} represents the free energy which is necessary for yielding to occur. Since this probability is less than the probability $P_{B\to A} = \exp(-F_{BA}/RT)$ for a yielded chain segment to recover to its initial structure (F_{BA} being the free energy), the recovery prevails.

Fig. 4 Unsymmetrical free energy barrier; F_{AB} and F_{BA} represent the activation free energies related to the passage of a chain segment from the initial state A to the deformed one B and the reverse

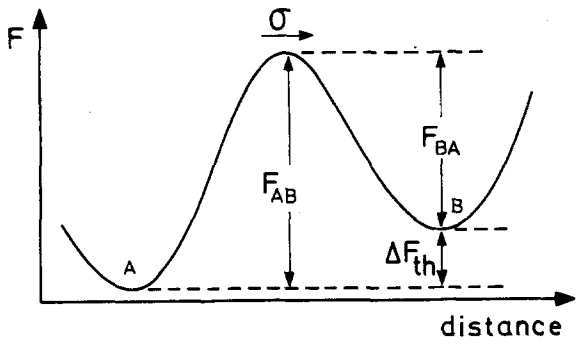

This model then predicts that a limiting stress exists for yielding below which there is no yielding and above which there is a finite rate of yielding.

In order to determine this threshold stress, let us consider the effect of an external stress σ (see Fig. 4) on the two probabilities mentioned above. They become

$$P_{A\to B} = \exp\left(-\frac{F_{AB} - W_\sigma}{RT}\right) \tag{4}$$

$$P_{B\to A} = \exp\left(-\frac{F_{BA} + W_\sigma}{RT}\right) \tag{5}$$

where W_σ denotes the stress work.

Both probabilities must be equal under the action of the threshold stress σ_{th}. Therefore,

$$W_{\sigma_{th}} = \frac{F_{AB} - F_{BA}}{2} = \frac{\Delta F_{th}}{2}, \tag{6}$$

where $W_{\sigma th}$ and ΔF_{th} denote the work and the free energy related to the threshold yield behavior.

As a result, when $W_\sigma < W_{\sigma th}$, yield deformation is hindered because $P_{B\to A} > P_{A\to B}$. On the contrary, when $P_{A\to B} > P_{B\to A}$, yield deformation occurs. It follows that σ_{th}, the stress related to W_{th}, has the character of a threshold stress from which deformation may begin.

When yield occurs, let ε_0 be the elementary deformation (often taken equal to unity [16]), then the strain-rate at yield is given by

$$\dot{\varepsilon} = \varepsilon_0 \cdot J_0 \cdot P_{A\to B}, \tag{7}$$

and the yield stress may be expressed as

$$\frac{\sigma}{T} = A\left(\ln\left(\frac{\dot{\varepsilon}}{\varepsilon_0 J_0}\right) + \frac{F_{AB}}{RT}\right), \tag{8}$$

as in the Ree–Eyring approach where a single process is implied (J_0 denoting the frequency factor).

It follows that parameter A may be written

$$A = \frac{R}{\varepsilon_0 V_0}, \tag{9}$$

where V_0 is the activation volume.

Although the free energy values differ in Eqs. (6) and (8), it will be assumed that the same activation volume is implied, the stress being equal to or higher than the threshold stress. This assumption will be supported further on.

Adjustment of the parameters

For clarity, above 100 °C, let us distinguish range *s* and range th related to the strain-rate dependent and to the threshold behavior respectively.

Within range s

Coming back to Fig. 3, let us consider the strain-rate dependent data at temperatures from 130° to 150 °C and assume that a single process (process 0) is acting, governed by Eq. (8), rewritten as

$$\frac{\sigma_0}{T} = A\left(\ln(2C\dot{\varepsilon}) + \frac{Q_{AB}}{RT}\right), \tag{10}$$

where C includes the entropy term of the free energy F_{AB}. The best fit parameters are given in Table 3. Let us point out that the activation enthalpy Q_{AB} is in this case evaluated from the horizontal distance between the straight lines.

The activation volume calculated from parameter A, the slope of the straight lines, using Eq. (9), is also given in Table 3.

The present results led us to reanalyze data related to process 1. The straight lines belonging to isothermal curves at 50°, 80°, 100°, and 120 °C, corresponding to this process, represent the variation of the sum of the stresses σ_0 and σ_1 and not σ_1 alone. The related activation energy must then be recalculated, a value of 268 kJ/mole is found, much lower than 435 kJ/mole evaluated previously.

Within range th

From (6), the proposed model accounts for a threshold stress given by

$$\sigma_{th} = \frac{\Delta F_{th}}{2\varepsilon_0 V_0} = \frac{\Delta Q_{th}}{2\varepsilon_0 V_0} - T\frac{\Delta S_{th}}{2\varepsilon_0 V_0}, \tag{11}$$

where Q_{th} and ΔS_{th} denote the enthalpy and entropy parts of the free energy ΔF_{th}, respectively. Therefore, according to this model, a linear dependence on T must be found for σ_{th}, the value of which must decrease when T increases.

Table 3 Constant parameters related to the threshold (range th) and the adjacent strain-rate dependent process (range s)

Zone th	$\Delta Q_{th} = 535$ kJ/mole	$\Delta S_{th} = 1137$ J/molK
zone s	$Q_{AB} = 652$ kJ/mole	$A = 2{,}17.10^{-3}$ MPa/K $\varepsilon_0 V_0 = 3900$ cm^3/mol

The data obtained at 140°, 145°, and 150 °C fit the following relation

$$\sigma_{th} = 70\left(1 - \frac{T}{470}\right)\text{MPa}, \tag{12}$$

the form of which is in agreement with Eq. (11). Parameters ΔS_{th} and Q_{th} may then be calculated using (11) and (12) and the value of $\varepsilon_0 V_0$ in Table 3. The computed values are also listed in Table 3.

Deformation process

Proposed mechanism

Within ranges th and *s*, the amorphous phase of the polymer is considered to be in the rubbery state, as the deformation contribution of processes 2 and 3, probably related to the upper and the lower glass transitions, have vanished. Therefore, it will be assumed here that yield deformation results from molecular motions taking place in the crystalline phase.

As previously proposed by Flory and Yoon [17] and by Takahashi et al. [18], it will be considered that yielding consists in a stress-induced melting followed by a recrystallization.

It will be assumed here that the elementary melting process affects a chain segment located between two folds. Figure 5 represents the considered mechanism: a chain segment between two folds melts under the action of the yield stress (a), is tilted in the stress direction (b), and crystallizes anew in the same direction (c).

Checking

In order to check that within both ranges, the deformation process is consistent with the stress-induced melting of

Fig. 5 Schematic representation of the deformation mechanism occurring at yield and consisting in melting of a chain segment located between two folds (a), tilting of this segment in the stress direction (b) and recrystallization (c)

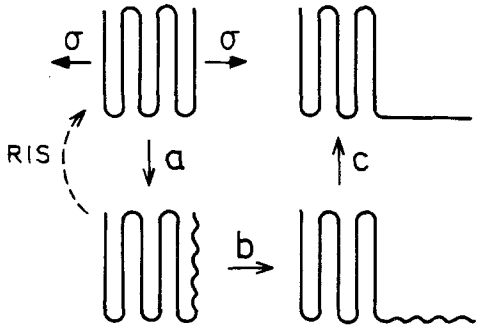

a crystalline segment located between two folds, let us calculate the length of such a segment. Two different ways will be followed related to ranges *s* and *th*, respectively.

1) *From parameter A (range s)*:

Let n be the number of carbons of the main chain implied in the deformation yield process. The weight of a crystalline segment of n carbons is $n.M/2$ where M denotes the molecular weight of the monomer (CH_2–CF_2). Assuming that yielding of crystalline layers implies deformation of some amorphous material, the involved polymer weight is $n\frac{M}{2}\frac{1}{\chi}$ where χ denotes the crystallinity.

Therefore, the activation volume can be expressed by

$$V_0 = \frac{\frac{n}{2}M}{\rho\chi}, \tag{13}$$

where ρ denotes the density of the polymer. From Eq. (9) and (13) and Tables 2 and 3, by assuming that $\varepsilon_0 \simeq 1$, a value $n = 121$ is obtained.

2) *From the value of ΔS_{th} (range th)*:

The entropy of the process is linked to the number of configurations P through

$$\Delta S_{th} = R\ln P . \tag{14}$$

Since two "gauche" and one "trans" conformations exist, it follows that

$$P = 3^n , \tag{15}$$

which gives $n = 125$; a value close to the one determined in range s.

Such a result implies that the same activation volume may be considered in both ranges, as previously assumed. Moreover, the same n value involves equal values of the entropy term in both ranges.

The considered chain segment is set along the z axis of the unit cell characterized by a lattice constant equal to 4,62 Å [19]. As the unit cell contains two monomers, the length of this segment of 125 carbons reaches 144 Å which is of the same magnitude as the crystalline lamellae thickness.

Let W_m denote the melting heat of the polymer written as

$$W_m = \chi h \rho V_0 . \tag{16}$$

This melting heat must then equal the activation enthalpy Q_{th} if melting really occurs at yield. Assuming that

$$W_m = Q_{th} , \tag{17}$$

and taking (16) and Tables 2 and 3 into account, a value of $V_0 = 4960\ cm^3$ is found, which is consistent with that of $3900\ cm^3$ obtained from (9) with $\varepsilon_0 \simeq 1$.

The assumed stress-induced melting is therefore supported by such results and implies that an increase in crystallinity or in the lamellae thickness raise the threshold stress or the yield stress in range *s*, respectively. Moreover, it results from this deformation process that positions A and B on the free energy curve of Fig. 4 are related to the crystalline and the amorphous state respectively.

Yield strain aspects

Creep curves

In order to check the threshold character of σ_{th} and the validity of Eq. (12), creep curves were carried out below and in the vicinity of this stress. Figure 6 gives an example of a creep curve performed at 100 °C below the threshold stress which reaches 14 MPa at this temperature, as calculated from (12). It can be seen from the shape of this curve that during the test, the strain-rate decreases continuously even after 2 months; deformation remains homogeneous.

At the threshold stress and within range *s*, creep curves exhibit a well defined inflection beyond which necking occurs at a strain of about 40%. The curve of Fig. 7 is an example.

Fig. 6 Creep curve obtained at 100 °C below the threshold stress. The engineering stress is equal to 11 MPa

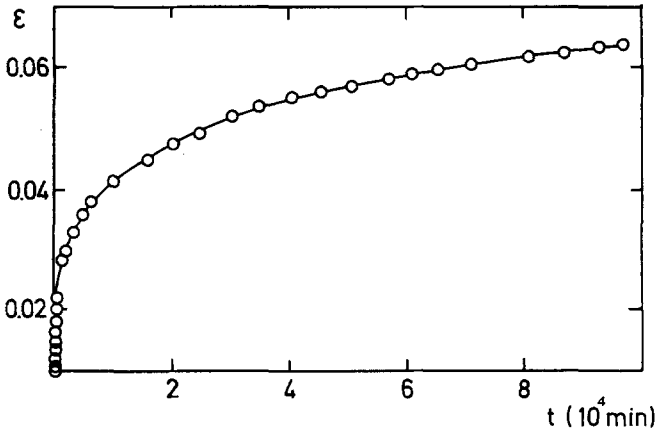

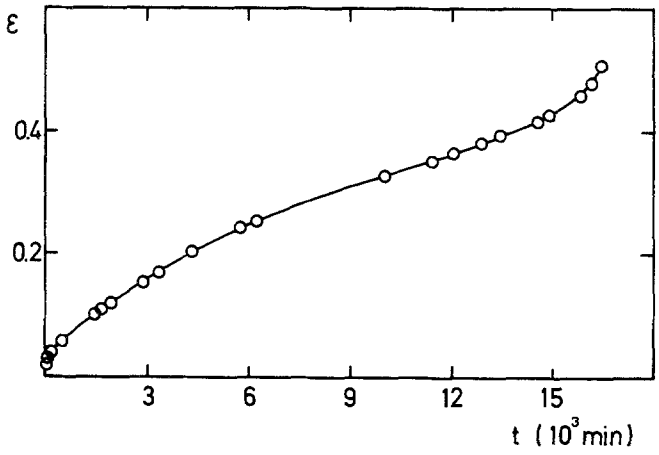

Fig. 7 Creep curve obtained at 100 °C at the threshold stress. The engineering stress is equal to 14 MPa

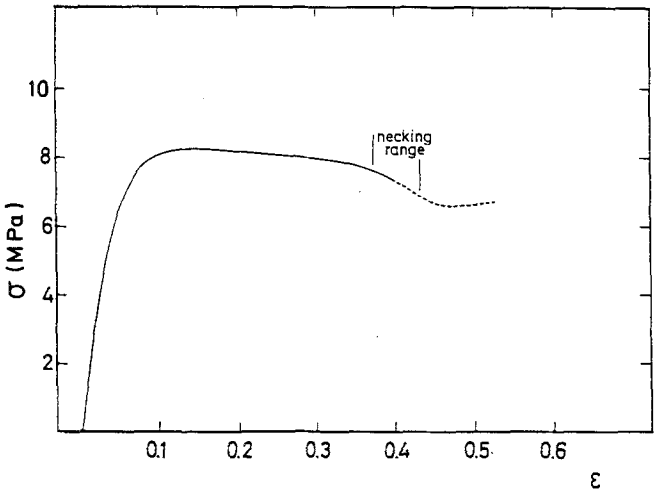

Fig. 8 Tensile curve obtained at 145 °C at a strian-rate of $4{,}17.10^{-3}\,s^{-1}$

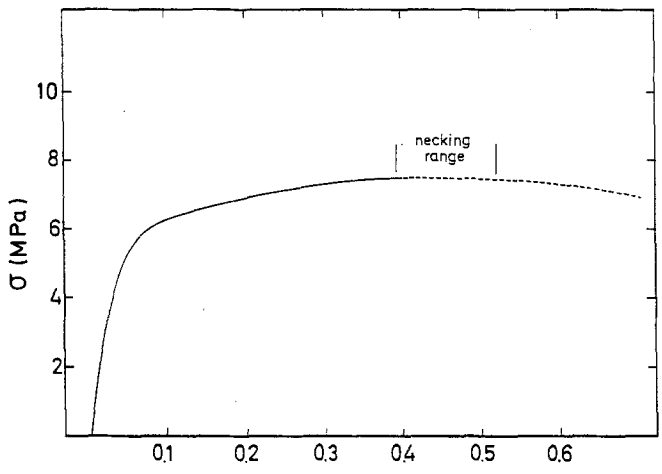

Fig. 9 Tensile curve obtained at 145° at a strain-rate of $2{,}08.10^{-4}\,s^{-1}$

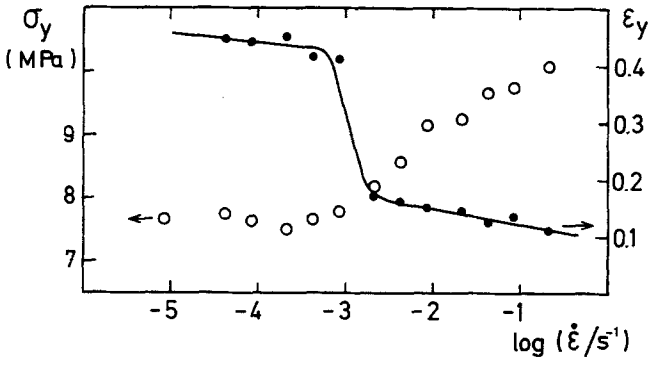

Fig. 10 Yield stress and yield strain versus the logarithm of stain-rate at 145 °C (tensile tests)

Tensile curves

Within range th, ε_y, the strain related to the engineering yield stress, reaches about 40% (see the tensile stress-strain curve given in Fig. 9) and the sample necks beyond this point.

Within range *s*, ε_y reaches 10%; the graph of Fig. 8 is an example of the related stress-strain curve. We observed that necking occurs at a strain of 40% as within range th. Beyond the yield point, but well before necking, the stress decreases continuously. Such a behavior could be attributed to softening effects produced by rejuvenation, as proposed previously [20].

In Fig. 10, we see the quantitative difference in the strain ε_y related to the maximum of the engineering tensile curve within ranges th and s respectively. ε_y is given versus the logarithm of strain-rate at 145 °C. As can be seen on the graph, the yield strain does not depend on the strain-rate within range th.

Conclusions

1) At least four rate processes operating in parallel may be needed to describe the tensile yield behavior of PVDF over a wide range of strain-rates and temperatures, using the Ree–Eyring approach. The two lowest temperature processes are associated with the double glass transition exhibited by this polymer, while the highest temperature process is related to a stress-induced melting occurring in the crystalline phase.

2) The Ree–Eyring theory must be modified to take into account the case where a threshold yield stress is observed by assuming an unsymmetrical free energy barrier for the rate process instead of a symmetrical one.
3) A single rate process is effective at high temperatures related to the melting of a chian segment containing 125 carbon atoms, i.e., about the length between two folds.
4) Such a model allows the level of the threshold stress to be determined as a function of the test temperature and the proposed deformation mechanism necessarily implies that this threshold stress increases with crystallinity.

Acknolwedgements Grateful acknowledgement is given to Mrs. C. Bauwens-Crowet, Chef de Travaux, for her helpful comments, discussions and suggestions, and to Mr. B. Triest for his efficient assistance throughout the experimental work. The authors are also pleased to express their appreciation to Solvay and Co. for their support of this research.

References

1. Ree T, Eyring H (1958) Rheology vol II chap III
2. Bauwens-Crowet C, Bauwens J-C (1969) J of Polym Sc A2 7:735
3. Bauwens-Crowet C (1973) J of Mat Sci 8:968
4. Roetling JA (1965) Polymer 6:311
5. Roetling JA (1965) Polymer 6:615
6. Roetling HA (1966) Polymer 7:303
7. Truss RW, Clarke PL, Duckett DA, Ward IM (1984) J of Polym Sci 22:191
8. Bauwens J-C (1971) J of Polym Sci C33:123
9. Bauwens J-C (1972) J of Mat Sci 7:577
10. Leonard C, Hallary JL, Monnerie L, Micheron F (1984) Polym Bulletin 11:195
11. Kalfoglou NK, Leverne-Williams H (1973) J of Appl Polym Sci 17:3367
12. Clément J-L (1989–1990) Travail de Fin d'Etudes, Université Libre de Bruxelles
13. Nagakawa K, Ishida J (1973) J of Polym Sci 11:1503
14. Bauwens-Crowet C, Bauwens J-C, Homes G (1969) J of Polym Sci A2 7:735
15. Matz DJ, Guldemont WG, Cooper SL (1972) J of Polym Sci Polym Phys Ed 10:1917
16. Bauwens J-C (1981) Polymer 21:699
17. Flory PJ, Yoon DY (1978) Nature 272:226
18. Takahashi Y, Zakoh T, Hanatani N (1992) Colloid Polym Sci 269:781
19. Hasegawa R, Takahashi Y, Chatani Y, Tadokoro H (1972) Polymer J3:600
20. Bauwens J-C (1992) Colloid Polym Sci 270:537
21. Haward RN, Thackray G (1968) Proc Roy Soc A302:453